Gravitational wave observations with PTA, can cosmic strings explain the signal?

(A cosmologist point of view)

Pierre Auclair

CP3 Seminar, December 12 2023

Cosmology, Universe and Relativity at Louvain (CURL)
Institute of Mathematics and Physics
Louvain University, Louvain-la-Neuve, Belgium

Outline

Introduction to pulsar timing
(Cosmologist point of view)

Hellings and Downs correlations

Data analysis and results

Cosmic string interpretation

Conclusion

Introduction to pulsar timing

(Cosmologist point of view)

- Neutron stars are **compact stars** with very **short rotational period** and extreme **magnetic fields**

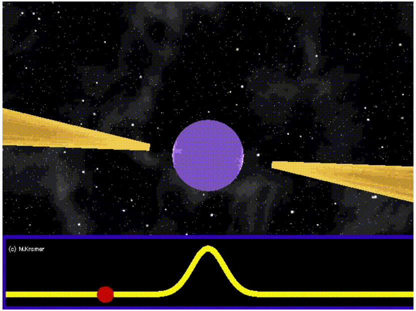

Introduction to pulsars

- Neutron stars are **compact stars** with very **short rotational period** and extreme **magnetic fields**
- Generally, the magnetic axis is not aligned with the spin axis, so radiation is swept through space.

  $\Longrightarrow$ Analogous to a lighthouse

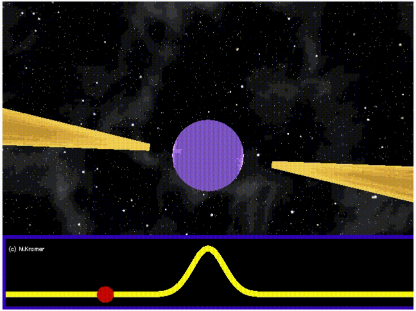

- Neutron stars are **compact stars** with very **short rotational period** and extreme **magnetic fields**
- Generally, the magnetic axis is not aligned with the spin axis, so radiation is swept through space.
  $\implies$ Analogous to a lighthouse
- They appear to the observer as pulses, separated by a fixed period that equals the spin

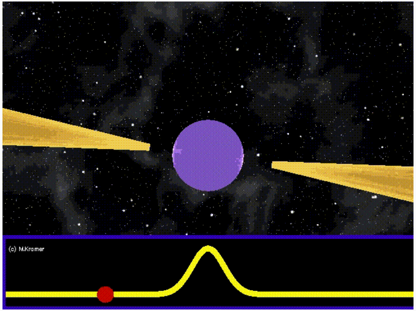

Pulse profiles

Pulse profiles vary across observing frequencies

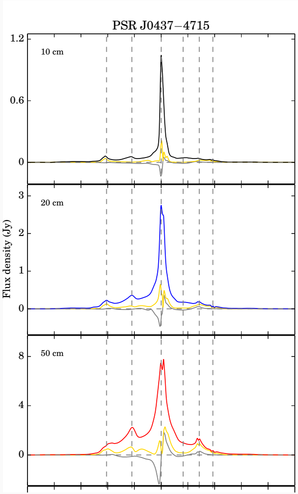

Pulsars studied in Parkes Pulsar Timing Array Dai et al. 2015

Pulse profiles

Pulse profiles vary across observing frequencies

- Pulse profiles tend to get sharper at higher frequencies...

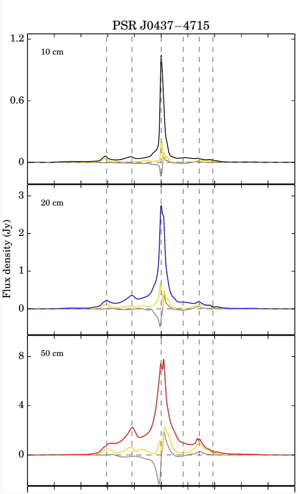

Pulsars studied in Parkes Pulsar Timing Array Dai et al. 2015

Pulse profiles

Pulse profiles vary across observing frequencies

- Pulse profiles tend to get sharper at higher frequencies...
- but the noise level increases due to the pulsar's steep spectrum

Most pulsar timing are carried around 1.4 GHz

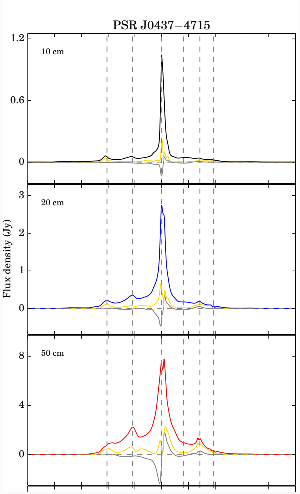

Pulsars studied in Parkes Pulsar Timing Array Dai et al. 2015

Pulse profiles

Pulse profiles vary across observing frequencies

- Pulse profiles tend to get sharper at higher frequencies...
- but the noise level increases due to the pulsar's steep spectrum

Most pulsar timing are carried around 1.4 GHz

Pulse profiles also vary across pulsars!

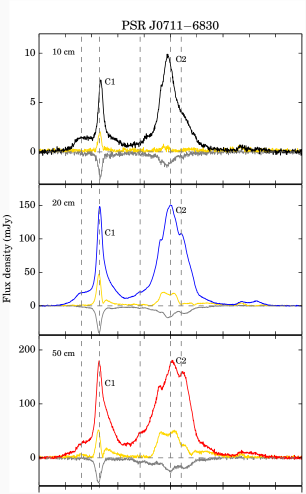

Pulsars studied in Parkes Pulsar Timing Array Dai et al. 2015

Pulse profiles

Pulse profiles vary across observing frequencies

- Pulse profiles tend to get sharper at higher frequencies...
- but the noise level increases due to the pulsar's steep spectrum

Most pulsar timing are carried around 1.4 GHz

Pulse profiles also vary across pulsars!

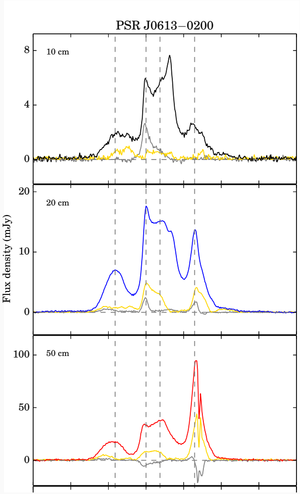

Pulsars studied in Parkes Pulsar Timing Array Dai et al. 2015

Radio emission from pulsars

The radio emission from pulsars has some intriguing properties

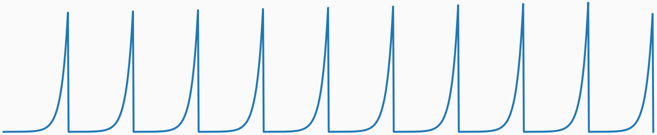

Radio emission from pulsars

The radio emission from pulsars has some intriguing properties

- Individual pulses change randomly from one pulse to the next, they are only stable on average (minutes to decades)

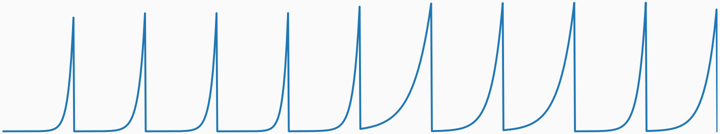

Radio emission from pulsars

The radio emission from pulsars has some intriguing properties

- Individual pulses change randomly from one pulse to the next, they are only stable on average (minutes to decades)
- Nulling: Pulsars that turn off only to reappear at some point after

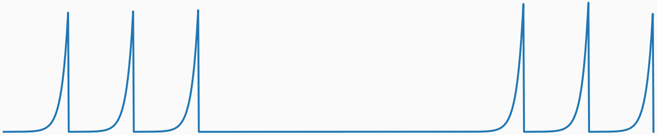

Radio emission from pulsars

The radio emission from pulsars has some intriguing properties

- Individual pulses change randomly from one pulse to the next, they are only stable on average (minutes to decades)
- Nulling: Pulsars that turn off only to reappear at some point after
- Moding: Pulsars that arbitrarily change between different fingerprints

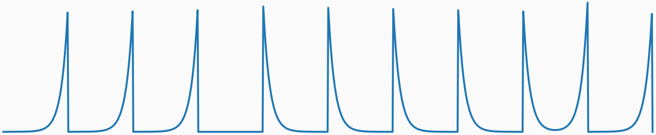

Radio emission from pulsars

The radio emission from pulsars has some intriguing properties

- Individual pulses change randomly from one pulse to the next, they are only stable on average (minutes to decades)
- Nulling: Pulsars that turn off only to reappear at some point after
- Moding: Pulsars that arbitrarily change between different fingerprints
- Drifting: Pulses appear to come a bit late after each rotation only to reset after a few dozen rotations

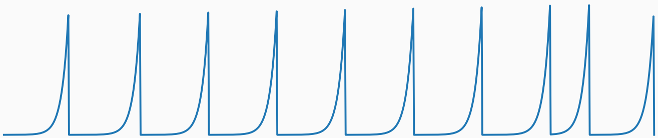

Different types of pulsars

Type of pulsar	Periods	Magnetic fields	Drift	Comment
Young	10 ms	10^{12} G	10^{-13}	Age < 1000 years

Different types of pulsars

Type of pulsar	Periods	Magnetic fields	Drift	Comment
Young	10 ms	10^{12} G	10^{-13}	Age < 1000 years
Slow	$0.1 - 10$ s	$10^{10} - 10^{13}$ G	10^{-14}	Age > 1000 years, less luminous

Different types of pulsars

Type of pulsar	Periods	Magnetic fields	Drift	Comment
Young	10 ms	10^{12} G	10^{-13}	Age < 1000 years
Slow	$0.1 - 10$ s	$10^{10} - 10^{13}$ G	10^{-14}	Age > 1000 years, less luminous
Millisecond (MSP)	$1 - 30$ ms	$< 10^{9}$ G	10^{-20}	NS spun-up through accretion from a binary companion

Different types of pulsars

Type of pulsar	Periods	Magnetic fields	Drift	Comment
Young	10 ms	10^{12} G	10^{-13}	Age < 1000 years
Slow	$0.1 - 10$ s	$10^{10} - 10^{13}$ G	10^{-14}	Age > 1000 years, less luminous
Millisecond (MSP)	$1 - 30$ ms	$< 10^{9}$ G	10^{-20}	NS spun-up through accretion from a binary companion

Millisecond pulsars (MSP) are at a sweet spot

Different types of pulsars

Type of pulsar	Periods	Magnetic fields	Drift	Comment
Young	10 ms	10^{12} G	10^{-13}	Age < 1000 years
Slow	$0.1 - 10$ s	$10^{10} - 10^{13}$ G	10^{-14}	Age > 1000 years, less luminous
Millisecond (MSP)	$1 - 30$ ms	$< 10^{9}$ G	10^{-20}	NS spun-up through accretion from a binary companion

Millisecond pulsars (MSP) are at a sweet spot

- small spin period $\implies$ pulse profiles can be obtained rapidly, in minutes

Type of pulsar	Periods	Magnetic fields	Drift	Comment
Young	10 ms	10^{12} G	10^{-13}	Age < 1000 years
Slow	$0.1 - 10$ s	$10^{10} - 10^{13}$ G	10^{-14}	Age > 1000 years, less luminous
Millisecond (MSP)	$1 - 30$ ms	$< 10^{9}$ G	10^{-20}	NS spun-up through accretion from a binary companion

Millisecond pulsars (MSP) are at a sweet spot

- small spin period $\implies$ pulse profiles can be obtained rapidly, in minutes
- very few MSPs have displayed anomalous emission properties (nulling, moding, drifting)

Different types of pulsars

Type of pulsar	Periods	Magnetic fields	Drift	Comment
Young	10 ms	10^{12} G	10^{-13}	Age < 1000 years
Slow	$0.1 - 10$ s	$10^{10} - 10^{13}$ G	10^{-14}	Age > 1000 years, less luminous
Millisecond (MSP)	$1 - 30$ ms	$< 10^{9}$ G	10^{-20}	NS spun-up through accretion from a binary companion

Millisecond pulsars (MSP) are at a sweet spot

- small spin period $\implies$ pulse profiles can be obtained rapidly, in minutes
- very few MSPs have displayed anomalous emission properties (nulling, moding, drifting)
- large angular momentum $\implies$ far more stable clocks than slow pulsars

Timing a pulse

How do we time a pulse? Why timing the peak is a bad idea:

- Noise $\implies$ peak is not well-resolved

Timing a pulse

How do we time a pulse? Why timing the peak is a bad idea:

- Noise $\implies$ peak is not well-resolved
- Position of the peak may vary across frequencies

Timing a pulse

How do we time a pulse? Why timing the peak is a bad idea:

- Noise $\implies$ peak is not well-resolved
- Position of the peak may vary across frequencies
- Precision needed for PTA δt is smaller than the sampling rate

Timing a pulse

How do we time a pulse? Why timing the peak is a bad idea:

- Noise $\implies$ peak is not well-resolved
- Position of the peak may vary across frequencies
- Precision needed for PTA δt is smaller than the sampling rate

Time of Arrivals (ToAs) are determined by matching pulses with template profiles:

- Standardized pulse shape, obtained after averaging over many rotations

Timing a pulse

How do we time a pulse? Why timing the peak is a bad idea:

- Noise $\implies$ peak is not well-resolved
- Position of the peak may vary across frequencies
- Precision needed for PTA δt is smaller than the sampling rate

Time of Arrivals (ToAs) are determined by matching pulses with template profiles:

- Standardized pulse shape, obtained after averaging over many rotations
- In theory this should be the noise-free pulse profile

Timing a pulse

How do we time a pulse? Why timing the peak is a bad idea:

- Noise $\implies$ peak is not well-resolved
- Position of the peak may vary across frequencies
- Precision needed for PTA δt is smaller than the sampling rate

Time of Arrivals (ToAs) are determined by matching pulses with template profiles:

- Standardized pulse shape, obtained after averaging over many rotations
- In theory this should be the noise-free pulse profile
- This operation needs a good knowledge of the pulsar's period

Timing a pulse

How do we time a pulse? Why timing the peak is a bad idea:

- Noise $\implies$ peak is not well-resolved
- Position of the peak may vary across frequencies
- Precision needed for PTA δt is smaller than the sampling rate

Time of Arrivals (ToAs) are determined by matching pulses with template profiles:

- Standardized pulse shape, obtained after averaging over many rotations
- In theory this should be the noise-free pulse profile
- This operation needs a good knowledge of the pulsar's period
- Template profiles may take advantage of the frequency-dependence of the pulses

Time of Arrivals (ToAs)

One ToA is obtained for each observation period:

- One arbitrary pulse is selected in the observation

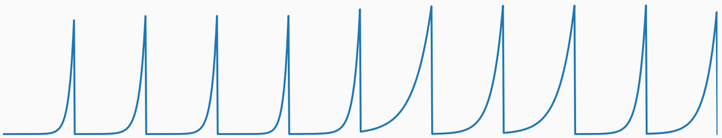

Time of Arrivals (ToAs)

One ToA is obtained for each observation period:

- One arbitrary pulse is selected in the observation
- Folding: average pulses modulo the pulse period to obtain an average pulse

Time of Arrivals (ToAs)

One ToA is obtained for each observation period:

- One arbitrary pulse is selected in the observation
- Folding: average pulses modulo the pulse period to obtain an average pulse
- Template matching: the pulse profile is cross-correlated with the template profile to obtain the phase of the observation

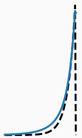

Time of Arrivals (ToAs)

One ToA is obtained for each observation period:

- One arbitrary pulse is selected in the observation
- Folding: average pulses modulo the pulse period to obtain an average pulse
- Template matching: the pulse profile is cross-correlated with the template profile to obtain the phase of the observation

The ToA combines the observation time stamp with the phase measurement

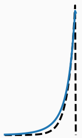

Transferring the observed times to the Pulsar

Accounting for all known propagation and geometric delays

$$t_{\mathrm{PSR}} = t_{\mathrm{obs}} - \Delta_{\odot} - \Delta_{ISM} - \Delta_{\mathrm{Bin}}$$

Transferring the observed times to the Pulsar

Accounting for all known propagation and geometric delays

$$t_{\rm PSR} = t_{\rm obs} - \Delta_\odot - \Delta_{ISM} - \Delta_{\rm Bin}$$

- $\Delta_\odot$ transferring to the Solar System barycenter. Accounts for a variety of effects: Earth's orbital and rotational velocity, mass distribution in the Solar System, Solar winds, parallax... Needs very precise ephemerides!

Transferring the observed times to the Pulsar

Accounting for all known propagation and geometric delays

$$t_{\mathrm{PSR}} = t_{\mathrm{obs}} - \Delta_{\odot} - \Delta_{ISM} - \Delta_{\mathrm{Bin}}$$

- $\Delta_{\odot}$ transferring to the Solar System barycenter. Accounts for a variety of effects: Earth's orbital and rotational velocity, mass distribution in the Solar System, Solar winds, parallax... Needs very precise ephemerides!
- Δ_{ISM} accounts for Interstellar propagation delays. Linked to the Dispersion Measure (DM), or the integrated electron content along the line-of-sight

$$\mathrm{DM} = \int_0^D n_e \, \mathrm{d}\ell$$

Transferring the observed times to the Pulsar

Accounting for all known propagation and geometric delays

$$t_{\rm PSR} = t_{\rm obs} - \Delta_{\odot} - \Delta_{ISM} - \Delta_{\rm Bin}$$

- $\Delta_{\odot}$ transferring to the Solar System barycenter. Accounts for a variety of effects: Earth's orbital and rotational velocity, mass distribution in the Solar System, Solar winds, parallax... Needs very precise ephemerides!
- Δ_{ISM} accounts for Interstellar propagation delays. Linked to the Dispersion Measure (DM), or the integrated electron content along the line-of-sight

$$\mathrm{DM} = \int_0^D n_e \, \mathrm{d}\ell$$

- $\Delta_{\rm Bin}$, for pulsars that are in binary systems

Building the timing model

Once the time of emission is determined, it can be converted to a rotational phase

$$\phi(t_{\mathrm{PSR}}) = \nu(t_{\mathrm{PSR}} - t_0) + \frac{1}{2}\dot{\nu}(t_{\mathrm{PSR}} - t_0)^2 + \dots$$

- ν is the pulsar's frequency
- $\dot{\nu}$ is the derivative of the pulsar frequency
- $\ddot{\nu}$ is usually too small in the case of MSPs

Building the timing model

Once the time of emission is determined, it can be converted to a rotational phase

$$\phi(t_{\mathrm{PSR}}) = \nu(t_{\mathrm{PSR}} - t_0) + \frac{1}{2}\dot{\nu}(t_{\mathrm{PSR}} - t_0)^2 + ...$$

- ν is the pulsar's frequency
- $\dot{\nu}$ is the derivative of the pulsar frequency
- $\ddot{\nu}$ is usually too small in the case of MSPs

In practice, there is an interplay between

- Construction of the template profile
- Determination of the timing model
- Knowledge of the propagation/geometric delays

Timing residuals

Difference between observed and predicted time of arrivals of the pulsars' radio pulses

$$\delta t_i = t_i^{\mathrm{obs}} - t_i^{\mathrm{TM}}$$

Timing residuals

Difference between observed and predicted time of arrivals of the pulsars' radio pulses

$$\delta t_i = t_i^{\mathrm{obs}} - t_i^{\mathrm{TM}}$$

Errors have an impact on timing residuals

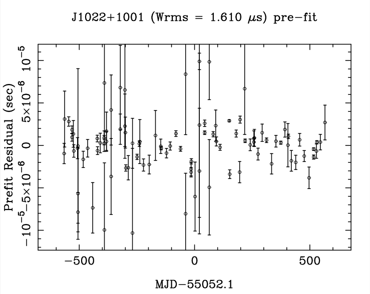

Typical PTA dataset Verbiest, Oslowski, and Burke-Spolaor 2021

Timing residuals

Difference between observed and predicted time of arrivals of the pulsars' radio pulses

$$\delta t_i = t_i^{\mathrm{obs}} - t_i^{\mathrm{TM}}$$

Errors have an impact on timing residuals

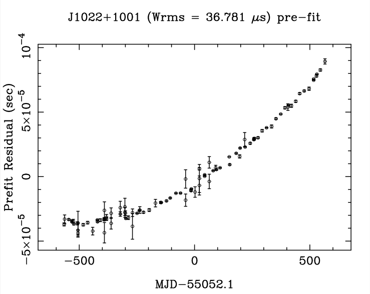

1% error on the spindown Verbiest, Oslowski, and Burke-Spolaor 2021

Timing residuals

Difference between observed and predicted time of arrivals of the pulsars' radio pulses

$$\delta t_i = t_i^{\mathrm{obs}} - t_i^{\mathrm{TM}}$$

Errors have an impact on timing residuals

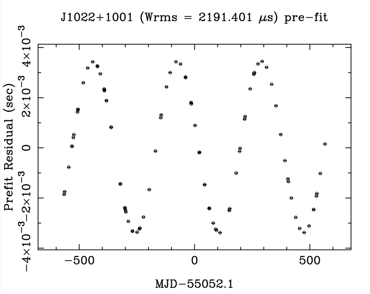

Positional offset of 0.1 arcsec in right ascension and declination Verbiest, Oslowski, and Burke-Spolaor 2021

Difference between observed and predicted time of arrivals of the pulsars' radio pulses

$$\delta t_i = t_i^{\mathrm{obs}} - t_i^{\mathrm{TM}}$$

Errors have an impact on timing residuals

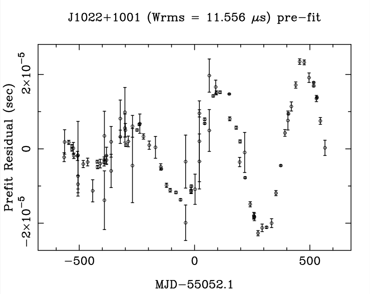

Proper motion is 10% incorrect Verbiest, Oslowski, and Burke-Spolaor 2021

Hellings and Downs correlations

Good reviews: Jenet and Romano 2015; Romano and Allen 2023

Time delay due to a GW (1/2)

- Time delay due to the passing of a GW

$$\Delta T(t) = \frac{1}{2c} u^i u^j \int_0^L \mathrm{d}s \, h_{ij}[\tau(s), \vec{\mathbf{x}}(s)]$$

Time delay due to a GW (1/2)

- Time delay due to the passing of a GW

$$\Delta T(t) = \frac{1}{2c} u^i u^j \int_0^L \mathrm{d}s\, h_{ij}[\tau(s), \vec{\mathbf{x}}(s)]$$

- Plane-wave decomposition of the GW

$$h_{ij}(t, \vec{\mathbf{x}}) = \int_{-\infty}^{+\infty} \mathrm{d}f \int \mathrm{d}\hat{\mathbf{k}} \sum_{A=+,\times} h_A(f, \hat{\mathbf{k}}) e_{ij}^A(\hat{\mathbf{k}}) \exp\left[i2\pi f(t - \hat{\mathbf{k}} \cdot \vec{\mathbf{x}}/c)\right]$$

Time delay due to a GW (1/2)

- Time delay due to the passing of a GW

$$\Delta T(t) = \frac{1}{2c} u^i u^j \int_0^L \mathrm{d}s \, h_{ij}[\tau(s), \vec{\mathbf{x}}(s)]$$

- Plane-wave decomposition of the GW

$$h_{ij}(t, \vec{\mathbf{x}}) = \int_{-\infty}^{+\infty} \mathrm{d}f \int \mathrm{d}\hat{\mathbf{k}} \sum_{A=+,\times} h_A(f, \hat{\mathbf{k}}) e_{ij}^A(\hat{\mathbf{k}}) \exp\left[i 2\pi f (t - \hat{\mathbf{k}} \cdot \vec{\mathbf{x}}/c)\right]$$

- At zeroth order, the photon propagates on a straight line

$$\vec{\mathbf{x}}(s) = \vec{\mathbf{r}}_1 + s\hat{\mathbf{u}}, \quad \tau(s) = t + (s - L)/c \quad \vec{\mathbf{r}}_2 = \vec{\mathbf{r}}_1 + L\hat{\mathbf{u}},$$

pulsar at $\hat{\mathbf{p}} = -\hat{\mathbf{u}}$

Time delay due to a GW (2/2)

$$\Delta T(t) = \int_{-\infty}^{+\infty} \mathrm{d}f \int \mathrm{d}\hat{\mathbf{k}} \sum_{A=+,\times} h_A(f,\hat{\mathbf{k}}) R^A(f,\hat{\mathbf{k}}) \exp\left[i2\pi f(t - \hat{\mathbf{k}}\cdot\vec{\mathbf{r}}_2/c)\right]$$

Response function

$$R^A(f,\hat{\mathbf{k}}) \equiv \frac{1}{2}u^i u^j e^A_{ij}(\hat{\mathbf{k}}) \, \frac{1}{i2\pi f} \, \frac{1}{1-\hat{\mathbf{k}}\cdot\hat{\mathbf{u}}} \left[\boxed{1} - \exp\left(-\frac{i2\pi f L}{c}(1-\hat{\mathbf{k}}\cdot\hat{\mathbf{u}})\right)\right]$$

- Earth term

Time delay due to a GW (2/2)

$$\Delta T(t) = \int_{-\infty}^{+\infty} \mathrm{d}f \int \mathrm{d}\hat{\mathbf{k}} \sum_{A=+,\times} h_A(f,\hat{\mathbf{k}}) R^A(f,\hat{\mathbf{k}}) \exp\left[i2\pi f(t - \hat{\mathbf{k}}\cdot\vec{\mathbf{r}}_2/c)\right]$$

Response function

$$R^A(f,\hat{\mathbf{k}}) \equiv \frac{1}{2} u^i u^j e_{ij}^A(\hat{\mathbf{k}}) \, \frac{1}{i2\pi f} \, \frac{1}{1-\hat{\mathbf{k}}\cdot\hat{\mathbf{u}}} \left[1 - \boxed{\exp\left(-\frac{i2\pi f L}{c}(1-\hat{\mathbf{k}}\cdot\hat{\mathbf{u}})\right)} \right]$$

- Earth term
- Pulsar term

$$\Delta T(t) = \int_{-\infty}^{+\infty} \mathrm{d}f \int \mathrm{d}\hat{\mathbf{k}} \sum_{A=+,\times} h_A(f,\hat{\mathbf{k}}) R^A(f,\hat{\mathbf{k}}) \exp\left[i2\pi f(t - \hat{\mathbf{k}}\cdot\vec{\mathbf{r}}_2/c)\right]$$

Response function

$$R^A(f,\hat{\mathbf{k}}) \equiv \frac{1}{2} u^i u^j e^A_{ij}(\hat{\mathbf{k}}) \, \frac{1}{i2\pi f} \boxed{\frac{1}{1-\hat{\mathbf{k}}\cdot\hat{\mathbf{u}}}} \left[1 \; - \; \exp\left(-\frac{i2\pi f L}{c}(1-\hat{\mathbf{k}}\cdot\hat{\mathbf{u}}) \right) \right]$$

- Earth term
- Pulsar term
- Breaks the $\hat{\mathbf{u}} \to -\hat{\mathbf{u}}$ symmetry, there is a difference if the photon is *surfing* the GW or *fight upstream*

Time delay due to a GW (2/2)

$$\Delta T(t) = \int_{-\infty}^{+\infty} \mathrm{d}f \int \mathrm{d}\hat{\mathbf{k}} \sum_{A=+,\times} h_A(f,\hat{\mathbf{k}}) R^A(f,\hat{\mathbf{k}}) \exp\left[i2\pi f(t - \hat{\mathbf{k}}\cdot\vec{\mathbf{r}}_2/c)\right]$$

Response function

$$R^A(f,\hat{\mathbf{k}}) \equiv \boxed{\frac{1}{2}u^i u^j e^A_{ij}(\hat{\mathbf{k}})} \frac{1}{i2\pi f} \frac{1}{1-\hat{\mathbf{k}}\cdot\hat{\mathbf{u}}} \left[1 \;-\; \exp\left(-\frac{i2\pi f L}{c}(1-\hat{\mathbf{k}}\cdot\hat{\mathbf{u}})\right) \right]$$

- Earth term
- Pulsar term
- Breaks the $\hat{\mathbf{u}} \to -\hat{\mathbf{u}}$ symmetry, there is a difference if the photon is *surfing* the GW or *fight upstream*
- Interaction between the photon and the GW polarizations

Short-arm limit $fL/c \ll 1$ (toy model for LIGO)

- The response function reduces to

$$R^A(f, \hat{\mathbf{k}}) = u^i u^j e^A_{ij}(\hat{\mathbf{k}}) \frac{L}{2c}$$

- Take a pulsar in the $\hat{\mathbf{z}}$ direction and $\cos(\theta) = \hat{\mathbf{k}} \cdot \hat{\mathbf{u}}$, then

$$\left|R^+(f, \hat{\mathbf{k}})\right| = \frac{L}{2c} \sin^2(\theta), \quad \left|R^\times(f, \hat{\mathbf{k}})\right| = 0$$

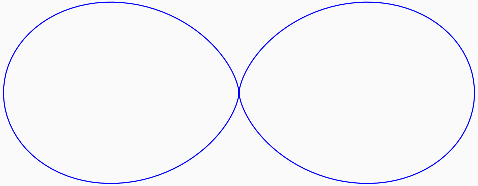

Reponse function $\left|R^+\right|$ for a pulsar located in the $+\hat{\mathbf{z}}$ direction.

Long-arm limit $fL/c \ll 1$ (PTA)

- We neglect the oscillatory pulsar term, provided $\hat{\mathbf{k}} \cdot \hat{\mathbf{u}} \neq 1$

$$R^A(f, \hat{\mathbf{k}}) = \frac{1}{2} u^i u^j e_{ij}^A(\hat{\mathbf{k}}) \frac{1}{i2\pi f} \frac{1}{1 - \hat{\mathbf{k}} \cdot \hat{\mathbf{u}}}$$

- Take a pulsar in the $\hat{\mathbf{z}}$ direction and $\cos(\theta) = \hat{\mathbf{k}} \cdot \hat{\mathbf{u}}$, then

$$\left| R^+(f, \hat{\mathbf{k}}) \right| = \frac{1}{4\pi f}(1+\cos\theta), \quad \left| R^\times(f, \hat{\mathbf{k}}) \right| = 0$$

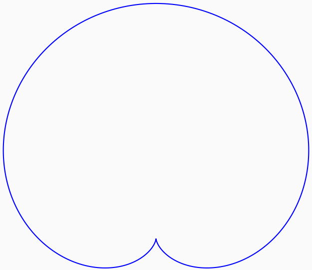

Reponse function $\left|R^+\right|$ for a pulsar located in the $+\hat{\mathbf{z}}$ direction.

Long-arm limit $fL/c \ll 1$ (PTA)

- We neglect the oscillatory pulsar term, provided $\hat{\mathbf{k}} \cdot \hat{\mathbf{u}} \neq 1$

$$R^A(f, \hat{\mathbf{k}}) = \frac{1}{2} u^i u^j e_{ij}^A(\hat{\mathbf{k}}) \frac{1}{i2\pi f} \frac{1}{1 - \hat{\mathbf{k}} \cdot \hat{\mathbf{u}}}$$

- Take a pulsar in the $\hat{\mathbf{z}}$ direction and $\cos(\theta) = \hat{\mathbf{k}} \cdot \hat{\mathbf{u}}$, then

$$\left| R^+(f, \hat{\mathbf{k}}) \right| = \frac{1}{4\pi f}(1 + \cos\theta), \quad \left| R^\times(f, \hat{\mathbf{k}}) \right| = 0$$

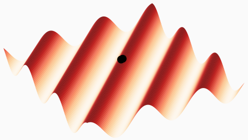

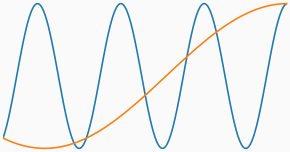

Stochastic background of GW

$$\left\langle h_A(f,\hat{\mathbf{k}})\right\rangle = 0, \quad \left\langle h_A(f,\hat{\mathbf{k}})h_{A'}(f',\hat{\mathbf{k}}')\right\rangle = \frac{1}{8\pi}H(f)\;\delta(f'-f)\;\;\delta_{AA'}\;\boxed{\delta^2(\hat{\mathbf{k}},\hat{\mathbf{k}}')}$$

- Statistically isotropic and homogeneous
- Stationary
- Unpolarized

Hellings and Downs correlation (1/2)

Stochastic background of GW

$$\left\langle h_A(f,\hat{\mathbf{k}})\right\rangle = 0, \quad \left\langle h_A(f,\hat{\mathbf{k}}) h_{A'}(f',\hat{\mathbf{k}}')\right\rangle = \frac{1}{8\pi} H(f) \boxed{\delta(f'-f)}\, \delta_{AA'} \;\; \delta^2(\hat{\mathbf{k}},\hat{\mathbf{k}}')$$

- Statistically isotropic and homogeneous
- Stationary
- Unpolarized

Stochastic background of GW

$$\left\langle h_A(f,\hat{\mathbf{k}})\right\rangle = 0, \quad \left\langle h_A(f,\hat{\mathbf{k}})h_{A'}(f',\hat{\mathbf{k}}')\right\rangle = \frac{1}{8\pi}H(f)\,\delta(f'-f)\,\boxed{\delta_{AA'}}\,\delta^2(\hat{\mathbf{k}},\hat{\mathbf{k}}')$$

- Statistically isotropic and homogeneous
- Stationary
- Unpolarized

Hellings and Downs correlation (1/2)

Stochastic background of GW

$$\left\langle h_A(f,\hat{\mathbf{k}})\right\rangle = 0, \quad \left\langle h_A(f,\hat{\mathbf{k}})h_{A'}(f',\hat{\mathbf{k}}')\right\rangle = \frac{1}{8\pi}H(f)\;\delta(f'-f)\;\;\delta_{AA'}\;\;\delta^2(\hat{\mathbf{k}},\hat{\mathbf{k}}')$$

- Statistically isotropic and homogeneous
- Stationary
- Unpolarized

- Photons coming from pulsars a and b have correlated time-delays

$$\langle \Delta T_a(t)\Delta T_b(t')\rangle = \int_{-\infty}^{\infty} \mathrm{d}f\,\mathrm{e}^{i2\pi f(t-t')}\,\Gamma_{ab}(f)H(f)$$

Hellings and Downs correlation (1/2)

Stochastic background of GW

$$\left\langle h_A(f,\hat{\mathbf{k}})\right\rangle = 0, \quad \left\langle h_A(f,\hat{\mathbf{k}})h_{A'}(f',\hat{\mathbf{k}}')\right\rangle = \frac{1}{8\pi}H(f)\;\delta(f'-f)\;\;\delta_{AA'}\;\;\delta^2(\hat{\mathbf{k}},\hat{\mathbf{k}}')$$

- Statistically isotropic and homogeneous
- Stationary
- Unpolarized

- Photons coming from pulsars a and b have correlated time-delays

$$\langle \Delta T_a(t)\Delta T_b(t')\rangle = \int_{-\infty}^{\infty} \mathrm{d}f\, \mathrm{e}^{i2\pi f(t-t')}\,\Gamma_{ab}(f)H(f)$$

- The correlation between two pulsars in encoded in

$$\Gamma_{ab}(f) \equiv \frac{1}{8\pi}\int \mathrm{d}\hat{\mathbf{k}}\sum_A R_a^A(f,\hat{\mathbf{k}})R_b^A(f,\hat{\mathbf{k}})\exp\left[-i2\pi f\,\hat{\mathbf{k}}\cdot(\vec{\mathbf{r}}_a-\vec{\mathbf{r}}_b)/c\right]$$

Hellings and Downs correlation (1/2)

Stochastic background of GW

$$\left\langle h_A(f,\hat{\mathbf{k}})\right\rangle = 0, \quad \left\langle h_A(f,\hat{\mathbf{k}}) h_{A'}(f',\hat{\mathbf{k}}')\right\rangle = \frac{1}{8\pi} H(f)\ \delta(f'-f)\ \ \delta_{AA'}\ \ \delta^2(\hat{\mathbf{k}},\hat{\mathbf{k}}')$$

- Statistically isotropic and homogeneous
- Stationary
- Unpolarized

- Photons coming from pulsars a and b have correlated time-delays

$$\langle \Delta T_a(t) \Delta T_b(t')\rangle = \int_{-\infty}^{\infty} \mathrm{d}f\, \mathrm{e}^{i2\pi f(t-t')}\, \Gamma_{ab}(f) H(f)$$

- The correlation between two pulsars in encoded in

$$\Gamma_{ab}(f) \equiv \frac{1}{8\pi}\int \mathrm{d}\hat{\mathbf{k}} \sum_A R_a^A(f,\hat{\mathbf{k}}) R_b^A(f,\hat{\mathbf{k}}) \cancel{\exp\left[-i2\pi f\, \hat{\mathbf{k}}\cdot(\vec{\mathbf{r}}_a - \vec{\mathbf{r}}_b)/c\right]}$$

Hellings and Downs correlation (2/2)

- Isolate the frequency-dependence

$$\Gamma_{ab}(f) = \frac{1}{12\pi^2 f^2}\Gamma_{ab}$$

Hellings and Downs correlation (2/2)

- Isolate the frequency-dependence

$$\Gamma_{ab}(f) = \frac{1}{12\pi^2 f^2}\Gamma_{ab}$$

- In the short-arm limit

$$\Gamma_{ab} = \frac{1}{2}P_2(\cos\gamma_{ab}) + \frac{\delta_{ab}}{2}$$

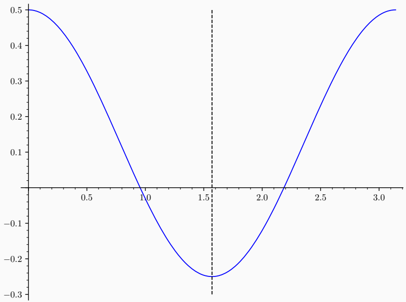

Hellings and Downs correlation (2/2)

- Isolate the frequency-dependence

$$\Gamma_{ab}(f) = \frac{1}{12\pi^2 f^2}\Gamma_{ab}$$

- In the short-arm limit

$$\Gamma_{ab} = \frac{1}{2}P_2(\cos\gamma_{ab}) + \frac{\delta_{ab}}{2}$$

- In the long-arm limit

$$\Gamma_{ab} = \frac{1}{2}+\frac{3}{2}\left(\frac{1-\cos\gamma_{ab}}{2}\right)\left[\ln\left(\frac{1-\cos\gamma_{ab}}{2}\right) - \frac{1}{6}\right]+\frac{\delta_{ab}}{2}$$

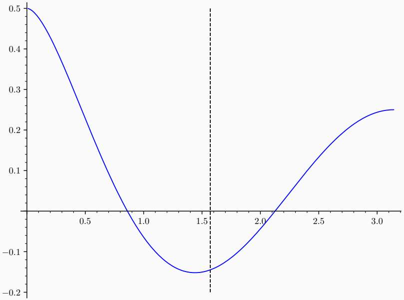

Data analysis and results

Sources of noise/signal

In addition to the deterministic components of the timing model, we have non-deterministic effects

Uncorrelated noises

- Pulse jitter
- Intrinsic spin noise
- Orbital Irregularities
- ISM Propagation Effects

Sources of noise/signal

In addition to the deterministic components of the timing model, we have non-deterministic effects

Uncorrelated noises

- Pulse jitter
- Intrinsic spin noise
- Orbital Irregularities
- ISM Propagation Effects

Correlated noises

- Imperfections in the reference clock
  $\Longrightarrow$ monopole
- Errors in Solar-System ephemerides
  $\Longrightarrow$ dipole
- Gravitational waves
  $\Longrightarrow$ quadrupole

Sources of noise/signal

In addition to the deterministic components of the timing model, we have non-deterministic effects

Uncorrelated noises

- Pulse jitter
- Intrinsic spin noise
- Orbital Irregularities
- ISM Propagation Effects

Correlated noises

- Imperfections in the reference clock
  $\Longrightarrow$ monopole
- Errors in Solar-System ephemerides
  $\Longrightarrow$ dipole
- Gravitational waves
  $\Longrightarrow$ quadrupole

All these noises can either be White (Uncorrelated in time) or Chromatic (Correlated in time)

Phenomenological noise models

Instead of modeling every noise individually, PTA construct a phenomenological model summarized in terms of the covariance matrix

$$C_{(ai)(bj)} = \mathcal{N}_{a,i}\delta_{ij}\delta_{ab} + C^{\mathrm{PSR}}_{a,ij}\delta_{ab} + \Gamma_{ab}C^{\mathrm{CRN}}_{ij}$$

[1] Hellings and Downs 1983.

Phenomenological noise models

Instead of modeling every noise individually, PTA construct a phenomenological model summarized in terms of the covariance matrix

$$C_{(ai)(bj)} = \mathcal{N}_{a,i}\delta_{ij}\delta_{ab} + C^{\mathrm{PSR}}_{a,ij}\delta_{ab} + \Gamma_{ab}C^{\mathrm{CRN}}_{ij}$$

- $\mathcal{N}_{a,i}$: White Noise covariance matrix
- $C^{\mathrm{PSR}}_{a,ij}$ Intrinsic red noise covariant matrix
- C^{CRN}_{ij} Common red noise covariance matrix
- Γ_{ab} the overlap function

[1] Hellings and Downs 1983.

Phenomenological noise models

Instead of modeling every noise individually, PTA construct a phenomenological model summarized in terms of the covariance matrix

$$C_{(ai)(bj)} = \mathcal{N}_{a,i}\delta_{ij}\delta_{ab} + C^{\mathrm{PSR}}_{a,ij}\delta_{ab} + \Gamma_{ab}C^{\mathrm{CRN}}_{ij}$$

- $\mathcal{N}_{a,i}$: White Noise covariance matrix
- $C^{\mathrm{PSR}}_{a,ij}$ Intrinsic red noise covariant matrix
- C^{CRN}_{ij} Common red noise covariance matrix
- Γ_{ab} the overlap function

In the case of Stochastic Background of GW[1]

$$\Gamma_{ab} = \frac{1}{2} + \frac{3}{2}\left(\frac{1-\cos\gamma_{ab}}{2}\right)\left[\ln\left(\frac{1-\cos\gamma_{ab}}{2}\right) - \frac{1}{6}\right] + \frac{\delta_{ab}}{2}$$

[1] Hellings and Downs 1983.

Bayesian statistics and model comparison

The likelihood for all observations is given by a Gaussian

$$p(\delta t|\eta) = \frac{1}{\sqrt{|2\pi C|}} \exp\left(-\frac{1}{2}\delta t^T C^{-1} \delta t\right)$$

To perform model comparison, we studied three approaches[a]

- Full method: sample parameters assuming a given SGWB spectrum

[a] Quelquejay Leclere et al. 2023.

Bayesian statistics and model comparison

The likelihood for all observations is given by a Gaussian

$$p(\delta t|\eta) = \frac{1}{\sqrt{|2\pi C|}} \exp\left(-\frac{1}{2}\delta t^T C^{-1} \delta t\right)$$

To perform model comparison, we studied three approaches[a]

- Full method: sample parameters assuming a given SGWB spectrum
- Resampling method: first sample parameters assuming $\Gamma_{ab} = \delta_{ab}$. Likelihood is factorized for each pulsar Then resample the posteriors assuming Γ_{ab}

[a] Quelquejay Leclere et al. 2023.

Bayesian statistics and model comparison

The likelihood for all observations is given by a Gaussian

$$p(\delta t|\eta) = \frac{1}{\sqrt{|2\pi C|}} \exp\left(-\frac{1}{2}\delta t^T C^{-1} \delta t\right)$$

To perform model comparison, we studied three approaches[a]

- Full method: sample parameters assuming a given SGWB spectrum
- Resampling method: first sample parameters assuming $\Gamma_{ab} = \delta_{ab}$. Likelihood is factorized for each pulsar Then resample the posteriors assuming Γ_{ab}
- Free spectrum: assume that all frequency bins are independent and obtain a posterior distribution for each of them. Adding new models is inexpansive

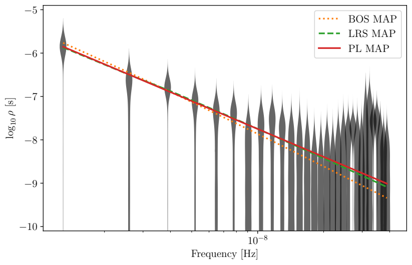

Posterior distributions in the 30 frequency bins Quelquejay Leclere et al. 2023

[a] Quelquejay Leclere et al. 2023.

Increasing evidence for GWs

- NANOGrav claims $3.5 - 4\sigma$ with 67 pulsars Agazie et al. 2023

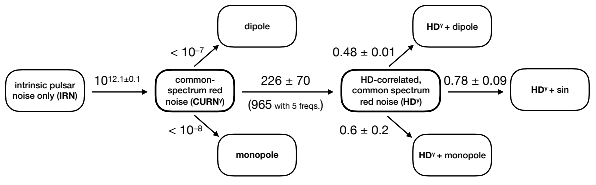

Bayes factors between models of correlated red noise in the NANOGrav 15-year data set Agazie et al. 2023

Increasing evidence for GWs

- NANOGrav claims $3.5 - 4\sigma$ with 67 pulsars Agazie et al. 2023
- EPTA claims $\geq 3\sigma$ with 25 pulsars Antoniadis et al. 2023a

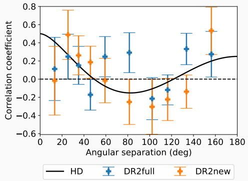

Constraints on the overlap reduction function from the optimal statistic Antoniadis et al. 2023a

Increasing evidence for GWs

- NANOGrav claims $3.5 - 4\sigma$ with 67 pulsars Agazie et al. 2023
- EPTA claims $\geq 3\sigma$ with 25 pulsars Antoniadis et al. 2023a
- PPTA claims 2σ with 30 pulsars Reardon et al. 2023

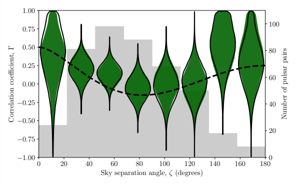

Measured spatial correlations as a function of the angular separation angle Reardon et al. 2023

Increasing evidence for GWs

- NANOGrav claims $3.5 - 4\sigma$ with 67 pulsars Agazie et al. 2023
- EPTA claims $\geq 3\sigma$ with 25 pulsars Antoniadis et al. 2023a
- PPTA claims 2σ with 30 pulsars Reardon et al. 2023
- CPTA claims 4.6σ with 57 pulsars Xu et al. 2023 but...

- Only 3 years of data
- Analysis carried at single frequencies
- Frequentist method (and argue that Bayesian method is biaised)
- They cannot distinguish HD at 4.6σ and dipole at 4.1σ

Interpretations

- Inspiraling supermassive black hole binaries (SMBHBs)
- Scalar-induced GWs
- First-order phase transitions
- Cosmic strings
- Domain walls

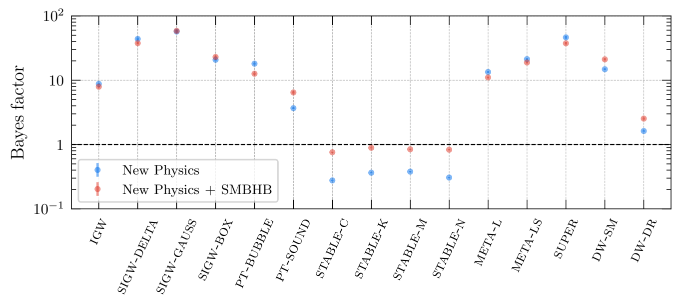

Bayes factors for the model comparisons between the new-physics interpretations and the interpretation in terms of SMBHBs alone Afzal et al. 2023

Cosmic string interpretation

What is a cosmic string ?

Cosmic string

A cosmic string is a one dimensional topological defect[1]. May form when the vacuum manifold has non-contractible loops.

Example: Mexican hat potential

- Vacuum manifold is a circle $\mathcal{M} = S^1$
- Fundamental group $\Pi_1(\mathcal{M}) = \mathbb{Z}$
- We expect strings to be formed in most models of spontaneous symmetry breaking[2]

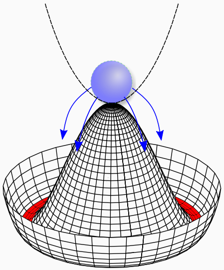

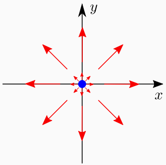

[1] Kibble 1976
[2] Jeannerot, Rocher, and Sakellariadou 2003

Cosmic string evolution

Energy scale	Width	Linear density
GUT : 10^{16} GeV	2×10^{-32} m	$G\mu \approx 10^{-6}$
3×10^{10} GeV	5×10^{-27} m	$G\mu \approx 10^{-17}$
10^{8} GeV	2×10^{-24} m	$G\mu \approx 10^{-22}$
EW : 100 GeV	2×10^{-18} m	$G\mu \approx 10^{-34}$

Nambu-Goto strings: one dimensional limit

- Width of the string very small compared to other length scales in the problem.
- String modeled as a line with mass per unit length $\mu \propto \eta^2$
- The Nambu-Goto action which minimizes the area swept by the string

$$\mathcal{S} = -\mu \int \mathrm{d}\tau \, \mathrm{d}\sigma \sqrt{-\det \gamma}$$

γ_{ab}: the induced metric on the string, τ is a time-like and σ a space-like coordinate along the string

Nambu-Goto strings in flat spacetime

Cosmic string dynamics

In flat spacetime, it satisfies a wave equation whose solution is

$$\mathbf{X}(t,\sigma) = \frac{1}{2}[\mathbf{a}(t-\sigma) + \mathbf{b}(t+\sigma)], \quad \mathbf{a}'^2 = \mathbf{b}'^2 = 1.$$

For a closed loop $\mathbf{X}(t,\sigma+\ell) = \mathbf{X}(t,\sigma)$: it oscillates with a period $T = \frac{\ell}{2}$.

Cosmic strings emit gravitational waves:

- Oscillation

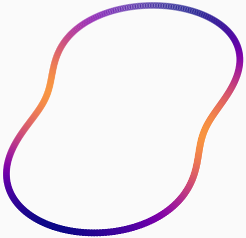

Nambu-Goto strings in flat spacetime

Cosmic string dynamics

In flat spacetime, it satisfies a wave equation whose solution is

$$\mathbf{X}(t,\sigma) = \frac{1}{2}[\mathbf{a}(t-\sigma) + \mathbf{b}(t+\sigma)], \quad \mathbf{a}'^2 = \mathbf{b}'^2 = 1.$$

For a closed loop $\mathbf{X}(t,\sigma+\ell) = \mathbf{X}(t,\sigma)$: it oscillates with a period $T = \frac{\ell}{2}$.

Cosmic strings emit gravitational waves:

- Oscillation
- Kink: when $\mathbf{X}'$ is not continuous

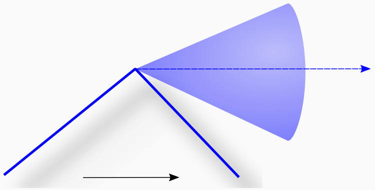

Nambu-Goto strings in flat spacetime

Cosmic string dynamics

In flat spacetime, it satisfies a wave equation whose solution is

$$\mathbf{X}(t,\sigma) = \frac{1}{2}[\mathbf{a}(t-\sigma) + \mathbf{b}(t+\sigma)], \quad \mathbf{a}'^2 = \mathbf{b}'^2 = 1.$$

For a closed loop $\mathbf{X}(t,\sigma+\ell) = \mathbf{X}(t,\sigma)$: it oscillates with a period $T = \dfrac{\ell}{2}$.

Cosmic strings emit gravitational waves:

- Oscillation
- Kink: when $\mathbf{X}'$ is not continuous
- Kink-kink collision

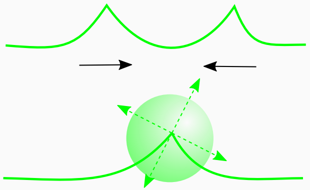

Nambu-Goto strings in flat spacetime

Cosmic string dynamics

In flat spacetime, it satisfies a wave equation whose solution is

$$\mathbf{X}(t,\sigma) = \frac{1}{2}[\mathbf{a}(t-\sigma) + \mathbf{b}(t+\sigma)], \quad \mathbf{a}'^2 = \mathbf{b}'^2 = 1.$$

For a closed loop $\mathbf{X}(t,\sigma+\ell) = \mathbf{X}(t,\sigma)$: it oscillates with a period $T = \frac{\ell}{2}$.

Cosmic strings emit gravitational waves:

- Oscillation
- Kink: when $\mathbf{X}'$ is not continuous
- Kink-kink collision
- Cusp: when $\dot{\mathbf{X}}^2 = 1$

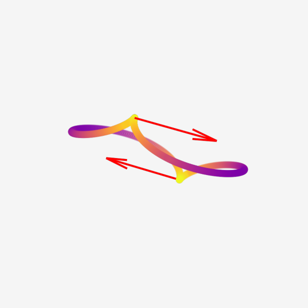

Nambu-Goto strings in flat spacetime

Cosmic string dynamics

In flat spacetime, it satisfies a wave equation whose solution is

$$\mathbf{X}(t,\sigma) = \frac{1}{2}[\mathbf{a}(t-\sigma) + \mathbf{b}(t+\sigma)], \quad \mathbf{a}'^2 = \mathbf{b}'^2 = 1.$$

For a closed loop $\mathbf{X}(t,\sigma+\ell) = \mathbf{X}(t,\sigma)$: it oscillates with a period $T = \dfrac{\ell}{2}$.

Cosmic strings emit gravitational waves:

- Oscillation
- Kink: when $\mathbf{X}'$ is not continuous
- Kink-kink collision
- Cusp: when $\dot{\mathbf{X}}^2 = 1$

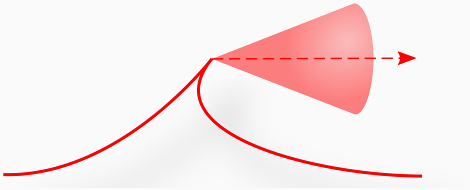

Model for the population of loops

- Long strings are stretched by the expansion of the Universe: $a(t)$
- They intersect each other and produce loops : $\mathcal{P}(\ell, t)$
- Loops decay by emitting gravitational waves : $\dot{E} = -\Gamma G \mu^2$

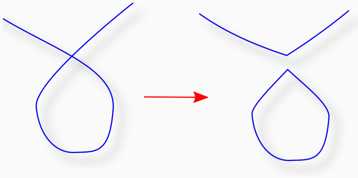

$$\frac{\partial}{\partial t}(a^3 \mathcal{N}) + \frac{\partial}{\partial \ell}\left[\frac{\mathrm{d}\ell}{\mathrm{d}t} a^3 \mathcal{N}\right] = a^3(t)\mathcal{P}(\ell, t)$$

The loop production function $\mathcal{P}$ is studied semi-analytically

The number of cosmic string loops $\mathcal{N}(\ell, t)$

Model for the population of loops

- Long strings are stretched by the expansion of the Universe: $a(t)$
- They intersect each other and produce loops : $\mathcal{P}(\ell, t)$
- Loops decay by emitting gravitational waves : $\dot{E} = -\Gamma G \mu^2$

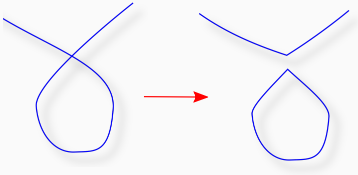

$$\frac{\partial}{\partial t}(a^3 \mathcal{N}) + \frac{\partial}{\partial \ell}\left[\frac{\mathrm{d}\ell}{\mathrm{d}t} a^3 \mathcal{N}\right] = a^3(t)\mathcal{P}(\ell, t)$$

The loop production function $\mathcal{P}$ is studied semi-analytically

- One-scale model Kibble 1985

$$t^5 \mathcal{P}(\ell, t) = C\delta\left(\frac{\ell}{t} - \alpha\right)$$

- Power-law loop production function Polchinski and Rocha 2006

$$t^5 \mathcal{P}(\ell, t) = C\left(\frac{\ell}{t}\right)^{2\chi - 3}$$

The stochastic background of gravitational waves

- The uncorrelated sum of all the GW signals produced by cosmic string loops constitutes a Stochastic Background of GW.
- We can estimate this background using energetic arguments

$$\Omega_{\mathrm{GW}}(\ln f) = \frac{8\pi G}{3\mathrm{H}_0^2} f \rho_{\mathrm{GW}}$$

$$\rho_{\mathrm{GW}}(f) = \int_0^{t_0} \frac{\mathrm{d}t}{[1+z(t)]^4} \mathrm{P}_{\mathrm{gw}}(t, f') \frac{\partial f'}{\partial f}$$

$$\mathrm{P}_{\mathrm{gw}}[t, f'] = G\mu^2 \sum_m \frac{2m}{f'^2} P_m \mathcal{N}\left(\frac{2m}{f'}, t\right)$$

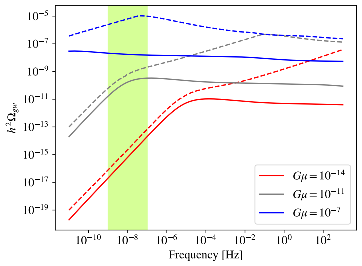

Quelquejay Leclere et al. 2023

Cosmic string interpretation: NANOGRAV

- NANOGRAV seems to favor Superstrings but...

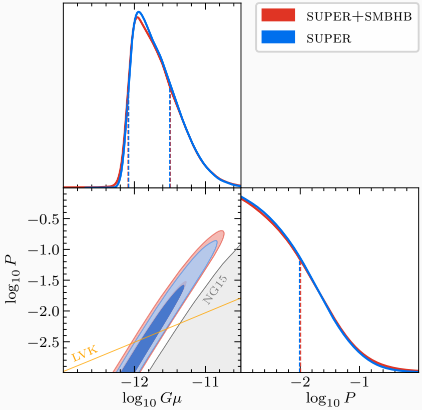

Afzal et al. 2023

Cosmic string interpretation: NANOGRAV

- NANOGRAV seems to favor Superstrings but...
- $\Omega_{\rm GW}(f) \to \Omega_{\rm GW}(f)/P$, with P intercommutation probability

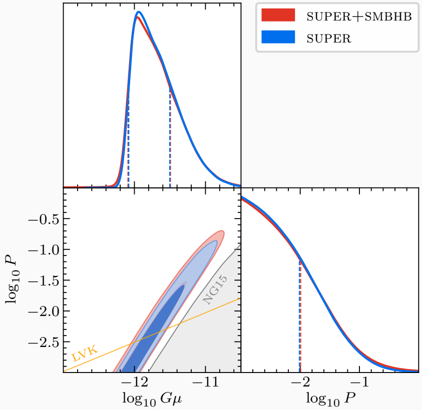

Afzal et al. 2023

- NANOGRAV seems to favor Superstrings but...
- $\Omega_{\mathrm{GW}}(f) \to \Omega_{\mathrm{GW}}(f)/P$, with P intercommutation probability
- Posterior for P covers the all prior

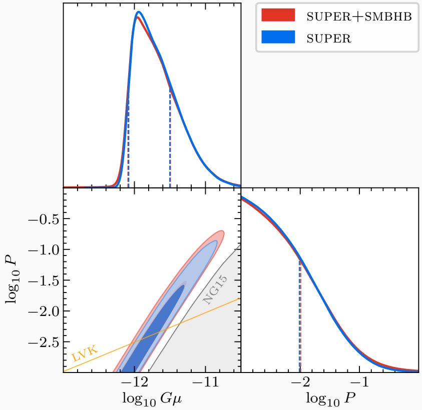

Afzal et al. 2023

Cosmic string interpretation: NANOGRAV

- NANOGRAV seems to favor Superstrings but...
- $\Omega_{\rm GW}(f) \to \Omega_{\rm GW}(f)/P$, with P intercommutation probability
- Posterior for P covers the all prior
- Scenario CS + SMBHB does not favor CS

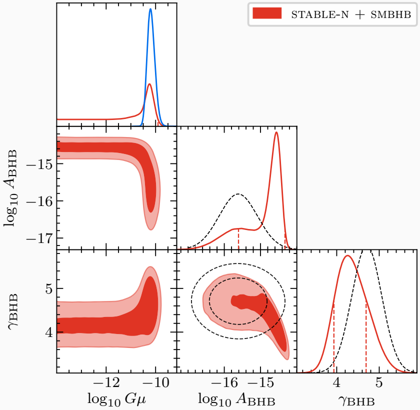

Afzal et al. 2023

Cosmic string interpretation: EPTA

- EPTA studied the BOS[a] and the LRS[b] models

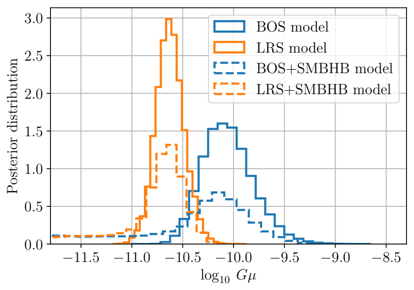

Antoniadis et al. 2023b

[a]Blanco-Pillado, Olum, and Shlaer 2014.
[b]Lorenz, Ringeval, and Sakellariadou 2010.
[c]Quelquejay Leclere et al. 2023.

Cosmic string interpretation: EPTA

- EPTA studied the BOS[a] and the LRS[b] models
- Values of $G\mu$ are comparable for both models

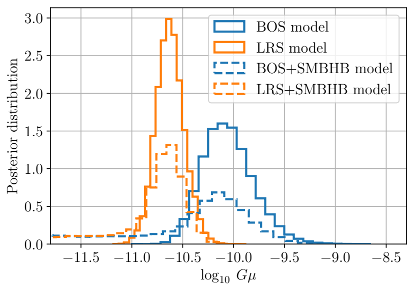

Antoniadis et al. 2023b

[a] Blanco-Pillado, Olum, and Shlaer 2014.
[b] Lorenz, Ringeval, and Sakellariadou 2010.
[c] Quelquejay Leclere et al. 2023.

Cosmic string interpretation: EPTA

- EPTA studied the BOS[a] and the LRS[b] models
- Values of $G\mu$ are comparable for both models
- EPTA does not favor a model in particular with $\mathcal{B} \approx 0.3$[c]

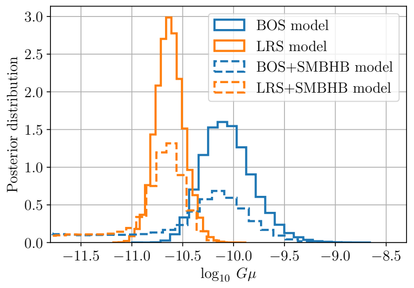

Antoniadis et al. 2023b

[a] Blanco-Pillado, Olum, and Shlaer 2014.
[b] Lorenz, Ringeval, and Sakellariadou 2010.
[c] Quelquejay Leclere et al. 2023.

Conclusion

Conclusion

- Pulsar Timing Arrays are exciting/difficult experiments: radio astronomy, high-energy astrophysics, solar-system, intense computing, cosmology...

Conclusion

- Pulsar Timing Arrays are exciting/difficult experiments: radio astronomy, high-energy astrophysics, solar-system, intense computing, cosmology...
- It is an exciting time for GW enthusiasts

Conclusion

- Pulsar Timing Arrays are exciting/difficult experiments: radio astronomy, high-energy astrophysics, solar-system, intense computing, cosmology...
- It is an exciting time for GW enthusiasts
- A GW stochastic background has (very probably) been detected!

Conclusion

- Pulsar Timing Arrays are exciting/difficult experiments: radio astronomy, high-energy astrophysics, solar-system, intense computing, cosmology...
- It is an exciting time for GW enthusiasts
- A GW stochastic background has (very probably) been detected!
- The interpretation is yet to be determined (Cosmic strings? Superstrings?)

Conclusion

- Pulsar Timing Arrays are exciting/difficult experiments: radio astronomy, high-energy astrophysics, solar-system, intense computing, cosmology...
- It is an exciting time for GW enthusiasts
- A GW stochastic background has (very probably) been detected!
- The interpretation is yet to be determined (Cosmic strings? Superstrings?)
- Looking forward to the International Pulsar Timing Array!

Conclusion

- Pulsar Timing Arrays are exciting/difficult experiments: radio astronomy, high-energy astrophysics, solar-system, intense computing, cosmology...
- It is an exciting time for GW enthusiasts
- A GW stochastic background has (very probably) been detected!
- The interpretation is yet to be determined (Cosmic strings? Superstrings?)
- Looking forward to the International Pulsar Timing Array!
- Software and datasets are available online

Thank you

References

Dai, S. et al. (2015). **"A study of multifrequency polarization pulse profiles of millisecond pulsars".** In: *Mon. Not. Roy. Astron. Soc.* 449.3, pp. 3223–3262. DOI: 10.1093/mnras/stv508. arXiv: 1503.01841 [astro-ph.GA].

Verbiest, J. P. W., S. Oslowski, and S. Burke-Spolaor (Jan. 2021). **"Pulsar Timing Array Experiments".** In: DOI: 10.1007/978-981-15-4702-7_4-1. arXiv: 2101.10081 [astro-ph.IM].

Jenet, Fredrick A. and Joseph D. Romano (2015). **"Understanding the gravitational-wave Hellings and Downs curve for pulsar timing arrays in terms of sound and electromagnetic waves".** In: *Am. J. Phys.* 83, p. 635. DOI: 10.1119/1.4916358. arXiv: 1412.1142 [gr-qc].

Romano, Joseph D. and Bruce Allen (Aug. 2023). **"Answers to frequently asked questions about the pulsar timing array Hellings and Downs correlation curve".** In: arXiv: 2308.05847 [gr-qc].

Hellings, R. w. and G. s. Downs (1983). **"UPPER LIMITS ON THE ISOTROPIC GRAVITATIONAL RADIATION BACKGROUND FROM PULSAR TIMING ANALYSIS".** In: *Astrophys. J. Lett.* 265, pp. L39–L42. DOI: 10.1086/183954.

Quelquejay Leclere, Hippolyte et al. (June 2023). **"Practical approaches to analyzing PTA data: Cosmic strings with six pulsars".** In: arXiv: 2306.12234 [gr-qc].

Agazie, Gabriella et al. (2023). **"The NANOGrav 15 yr Data Set: Evidence for a Gravitational-wave Background".** In: *Astrophys. J. Lett.* 951.1, p. L8. DOI: 10.3847/2041-8213/acdac6. arXiv: 2306.16213 [astro-ph.HE].

Antoniadis, J. et al. (June 2023a). **"The second data release from the European Pulsar Timing Array III. Search for gravitational wave signals".** In: arXiv: 2306.16214 [astro-ph.HE].

Reardon, Daniel J. et al. (2023). **"Search for an Isotropic Gravitational-wave Background with the Parkes Pulsar Timing Array".** In: *Astrophys. J. Lett.* 951.1, p. L6. DOI: 10.3847/2041-8213/acdd02. arXiv: 2306.16215 [astro-ph.HE].

Xu, Heng et al. (2023). **"Searching for the Nano-Hertz Stochastic Gravitational Wave Background with the Chinese Pulsar Timing Array Data Release I".** In: *Res. Astron. Astrophys.* 23.7, p. 075024. DOI: 10.1088/1674-4527/acdfa5. arXiv: 2306.16216 [astro-ph.HE].

Afzal, Adeela et al. (2023). **"The NANOGrav 15 yr Data Set: Search for Signals from New Physics".** In: *Astrophys. J. Lett.* 951.1, p. L11. DOI: 10.3847/2041-8213/acdc91. arXiv: 2306.16219 [astro-ph.HE].

Kibble, T. W. B. (1976). **"Topology of Cosmic Domains and Strings".** In: *J. Phys. A* 9, pp. 1387–1398. DOI: 10.1088/0305-4470/9/8/029.

Jeannerot, Rachel, Jonathan Rocher, and Mairi Sakellariadou (2003). **"How generic is cosmic string formation in SUSY GUTs".** In: *Phys. Rev. D* 68, p. 103514. DOI: 10.1103/PhysRevD.68.103514. arXiv: hep-ph/0308134.

Kibble, T. W. B. (1985). **"Evolution of a system of cosmic strings".** In: *Nucl. Phys. B* 252. Ed. by R. Baier and H. Satz. [Erratum: Nucl.Phys.B 261, 750 (1985)], p. 227. DOI: 10.1016/0550-3213(85)90596-6.

Polchinski, Joseph and Jorge V. Rocha (2006). **"Analytic study of small scale structure on cosmic strings".** In: *Phys. Rev. D* 74, p. 083504. DOI: 10.1103/PhysRevD.74.083504. arXiv: hep-ph/0606205.

Blanco-Pillado, Jose J., Ken D. Olum, and Benjamin Shlaer (2014). **"The number of cosmic string loops".** In: *Phys. Rev. D* 89.2, p. 023512. DOI: 10.1103/PhysRevD.89.023512. arXiv: 1309.6637 [astro-ph.CO].

Lorenz, Larissa, Christophe Ringeval, and Mairi Sakellariadou (2010). **"Cosmic string loop distribution on all length scales and at any redshift".** In: *JCAP* 10, p. 003. DOI: 10.1088/1475-7516/2010/10/003. arXiv: 1006.0931 [astro-ph.CO].

Antoniadis, J. et al. (June 2023b). **“The second data release from the European Pulsar Timing Array: V. Implications for massive black holes, dark matter and the early Universe”.** In: arXiv: 2306.16227 [astro-ph.CO].